D145
LMSC/D961899

(NASA-CR-175514) STS ATMOSPHERIC LUMINOSITIES Final Report (Lockheed Missiles and Space Co.) 24 p HC A02/MF A01 CSCL 22B

N85-21240

Unclas
G3/16 14511

STS ATMOSPHERIC LUMINOSITIES

NASW-3862

FINAL REPORT

S. B. Mende
Lockheed Palo Alto Research Laboratories
Palo Alto, CA 94304

5/14/84

ABSTRACT

During the STS-8 space shuttle mission special photographic and TV operations were carried out to record the properties of the spacecraft induced luminosities. One of these luminous phenomena is the quiescent vehicle glow which was photographed during the STS-8 mission with an image intensified photographic camera, with and without an objective grating. During the latter part of the mission the altitude of the shuttle was relatively low (120 n.m.=222 km) and unprecedentedly high intensity of the glow was observed. The crew reported that the glow was easily visible to the naked eye. The proper orientation of the shuttle with respect to the velocity vector and the objective grating permitted the exposure of good objective spectrum of the glow in the visible region. From the results it is clear that the spectrum appears to be a continuum as observed by the image intensifier objective grating camera. Qualitative examination of the data shows that there is very tail little glow in the wavelength range of 4300 to about 5000 angstroms. Above 5000 angstroms the glow becomes stronger towards the red and then it falls off towards higher wavelength and of the spectrum presumably because of the responsivity of the device. Three material samples were also exposed in the ram direction during the night side of the orbit and the glow surrounding the samples was photographed. The glow intensity varied depending on the nature of the sample surface. The other luminosity investigated by the STS-8 experiment was the thruster induced light. Thrusters were initiated individually and the resulting luminosities were recorded by photographic and television techniques. These results show that the largest optical disturbance is created by the downward firing tail thrusters (-ve pitch) presumably because these thrusters fire towards the orbiter wing which then thermalizes the exhaust gases by collisions. The thruster induced spacecraft glow was found to decay with a time constant which is 1/5 th of the time constant obtained on STS-3.

INTRODUCTION

The apparent vehicle glow of the space shuttle was detected during the flight of STS-3 (Banks et al. 1983). Although the shuttle glow was not specifically predicted it has now been associated with other spacecraft glow which was shown to surround free flier satellites such as the Atmospheric Explorer. (See Torr 1983, Yee and Abreu 1983).

Specific investigation of the shuttle glow was started on STS-4 when a transmission grating was mounted in front of a photogtraphic camera and several exposures were taken on orbit to make preliminary spectral measurements of the spacecraft glow (Mende et al. 1983a). The STS-4 experiment provided a single 400 second exposure photograph with glow spectral information. This image showed that the glow was observed predominantly in the far red to infrared region (6300-8000A) of the instrumental band pass (4300 - 8000A).

On STS-5 some of the properties of the shuttle glow were observed with an image intensifier camera. Comparison of the STS-3 (240 km) and STS-5 (305 km) photographs show that the intensity of the glow is about a factor of 3.5 brighter on the low altitude (STS-3) flight (Mende et al., 1983c). On STS-5 the orbiter was purposely rotated about the x axis in an experiment to observe the dependence of the intensity on the angle of incidence between the spacecraft surface normal and the velocity vector. For a relatively large angle between the velocity vector and the surface normal there was an appreciable glow, provided the surface is not shadowed by some other spacecraft structure. As the angle becomes less the glow intensifies. The grating experiments (STS-4 photography only, STS-5 image intensifier photography) provided a preliminary low resolution spectra of the spacecraft glow. Accurate wavelength calibrations of the STS-5 instrument permitted us to measure the spectrum and intensity of the earth's airglow. Comparisons with prior airglow measurements provides a great deal of confidence regarding the glow intensities obtained in the experiment (Mende et al., 1983b). Absolute responsivity calibration of the instrument was also performed by means of a laboratory standard source. Unique interpretation of the absolute spectra of the glow measurements on STS-5 were relatively difficult due to the large angle between the velocity vector and the glowing surfaces and due to the fact that the weak first order spectrum was superimposed on the bright earth's airglow. Nevertheless a weak spectra was obtained which shows a spectrally uniform glow. The photographic densities due to this glow were measured and compared to the absolute intensity measurements. This glow amounted to a few hundred Rayleighs per Angstrom with a spectrum rising towards the infrared. This rise is an interpretation of the apparent spectrally uniform photographic spectrum combined with the responsivity of the device which is falling rapidly towards the infrared.

Much speculation has taken place regarding the causes of the spacecraft glow. The first suggestions proposed that atmospheric O was recombining on the shuttle surfaces and the resulting O_2 was formed in an excited state. The resulting emissions would be expected to have the spectral signature of the O_2 Hertzberg bands mainly in the blue-ultra violet region of the spectrum. From the examination of the atmospheric explorer (AE) data earlier Torr et al. 1977 had suggested that the AE glow was due to NO_2 continuum. However, this suggestion is not consistent with the more recently published spectral data of the AE glow (Yee and Abreu 1983). Papadopolous (1983) suggested another a plasma mechanism for creating the spacecraft glow. This suggestion invokes the Alfven critical velocity ionization mechanism which should occur for neutrals which travel at velocities (perpendicular to B) corresponding to kinetic energy which is higher than the ionization potential of the particle. In the case of the shuttle an elastically scattered atmospheric atom or molecule would achieve high enough velocities for this process to take place. Even if this were not the key mechanism for the production of the glow this might prove significant in explaining some of the anomalous plasma conditions which were found on STS-3.

A phenomena, which is closely related to spacecraft glow and which may have very serious practical implications, is the intense emission generated by the the orbiter attitude control system. This phenomena was detected also on the STS-3 mission by Banks et al., 1983. The peak intensity of this emission is much greater than the intensity of the quiescent spacecraft ram glow. From a single photograph taken with an objective grating Mende et al., 1983, have attempted to infer that the spectra of this emission peaks strongly in the far red infrared region. The thruster glow was investigated by using the orbiter closed circuit television system on STS-3 and spectacular video sequences were recorded on the orbiter video recorders. It is suspected that the thruster glow is strong enough to cause serious stray light interference to engineering systems such as star sensors on orbiter launched vehicles.

The primary objectives of the STS-8 glow experiment objectives were to obtain a good high signal to noise ratio measurement of the optical spectrum of the glow on the shuttle tail. This required the stabilization of the orbiter in an attitude configuration in which the velocity vector was towards the starboard wing (orbiter y axis). This configuration assures that the atmospheric flow is impinging on the starboard side of the tail producing a luminous vertical "slit" for our objective grating spectrometer.

Another objective of the STS-8 experiment was to detect whether the intensity of the shuttle glow is dependent on the nature of the shuttle surface materials. For this purpose sample materials were attached to the remote manipulator system (RMS) arm and photographs were taken during flight when the velocity vector was straight up the payload bay (parallel to orbiter -z axis) and the material surfaces were exposed to the atmosphere.

The thruster induced luminosities were also investigated on the STS-8 mission by taking long exposure photographs and activating various thruster jets and thus recording the intensity of the emissions created by the various thrusters.

EXPERIMENT HARDWARE AND CALIBRATIONS

The flight hardware for the STS-8 mission consisted of the same hardware previously used on the STS-5 glow experiment (Mende et al.,1983b, Mende et al., 1983c). An optionally demountable objective grating (300 lines/mm) preceeded the camera lens (NIKON F/1.2 55 mm camera objective). The lens focused the image on the photocathode (S-25) of a VARO 25mm second generation inverter tube. The phosphor output of the inverter tube was lens coupled into a flight qualified NIKON photographic camera. This camera was mounted inside the orbiter in the aft flight deck window by means of a mounting bracket. A suitable black cloth window shade was used to exclude stray light from the orbiter cabin lights.

The image intensifier camera and grating system were calibrated in the laboratory prior to flight in a manner similar to the STS-5 flight (Mende et al., 1983c). In the calibration procedure exposures were taken with the grating intensifier camera of various test objects. One of these was a Hg light source which was blocked off to produce a narrow slit thus producing a set of spectral lines of known wavelength. The other was a pre-calibrated secondary standard continuum light source of known emissivity as a function of wavelength. This light source also had a set of built in apertures so that its intensity could be varied by a factor of 500 without changing the spectral content of the emitted light. The test exposures and the flight film will be microdensitometered and the results will be reduced to curves of density as a function of input light intensity for each wavelength and for each exposure duration.

Two photo sessions were scheduled during the mission. The flight crew reported that the intensity of the glow was strong enough to be clearly visible to the naked eye. This was the first report of the detection of the glow by the unaided eye. Presumably the unprecedented intensity of the glow was the result of the relatively low altitude (120 n.m.=222 km). In comparison the altitude of STS-3 was 135 n.m. (250 km) and STS-4 and STS-5 were both flown at 160 n.m. (297 km).

OBSERVATIONS AND RESULTS

In the first part of the experiment the orbiter velocity was aligned parallel to the orbiter -z axis (this direction is vertically up in the orbiter bay). The material samples were photographed with the intensifier camera without the grating. First samples mounted on the remote manipulator system (RMS) arm were photographed with varied exposure times. After that exposures were taken of the material samples mounted on trays in the orbiter bay. These samples were part of a material science experiment.

The material samples on the RMS arm were mounted in the form of four inch wide tapes. The layout of the tapes was selected to maximize the "limb glow" over the curvature of the cylindrical arm. The layout is illustrated photographically on Fig. 1. (top photograph) this picture was taken prior to flight. The samples are in the following sequence: kapton (polyimide), aluminum, black chem-glaze, aluminum, and kapton. The samples were repeated in order to avoid the possible ambiguity caused by the slightly different geometry of the different view angles of the samples.

Kapton was chosen because of its known high weight loss property in shuttle orbital environment, aluminum was chosen because its known stability and black chem-glaze (carbon filled urethane based matt black light absorbing paint) because of its application in low light level detecting devices. Image intensified (bottom) photograph of the the RMS arm with the material samples. The glow above the chem-glaze is stronger than the glow above the other materials. Aluminum glows the least. The kapton samples and their associate glow are indistinguishable from the covering material of the arm. This photograph is the first solid evidence that the spacecraft ram glow depends on the material surface properties of the spacecraft.

Analysis of the samples after the flight is in process at the time of writing this report. Preliminary results of this analysis show that increased material loss rates do not correspond with the higher glow intensities reported here. (Leger private communications, 1983).

The second objective of the experiment was to obtain a good signal to noise ratio objective spectrum of the tail glow. For this experiment the velocity vector was aligned with the orbiter y axis (this direction is in the direction of the starboard wing). Five exposures were taken with the grating in position and the lens set at F/2.8. The duration of the five exposures were 8, 4, 1, 1/4, and 1/15 second respectively. The one second duration exposure was reproduced in Fig 2. The glow illuminated the starboard side of the tail and the starboard engine pod. These can be observed most clearly in the right side of the picture where the zero order image is located. The horizontal streaks on the photographs are the first order images or spectra of stars. Some stars have both their zero order point images and their first order spectral streak images in the picture. The large diffuse image a little left of the center is the first order or spectral image of the glow. Approximate wavelength scale was superimposed on the frame.

From Figure 2 it is qualitatively evident that the shuttle glow is spectrally diffuse. It is also clear that there is very little glow in the wavelength range of 4300 to about 5000 angstroms. In the range above 5000 angstroms the glow becomes more intense falling off towards the higher end presumably due to the falling response of the image intensifier photocathode (Mende et al., 1983b).

In the spectral image of Figure ? there is an apparent line emission. This is evident because of the presence of a well defined image of the tail in first order. Since it is a well defined image its wavelength can be derived fairly accurately. Within the accuracy of the preliminary measurements the wavelength of the feature was found to be 7600 ±50 angstroms. This suggests that the observed emission is scattered airglow in the O_2 atmospheric airglow band at 7619. There is other evidence that this feature is not part of the spacecraft glow. Close examination of the figure will reveal that the first order image is equally bright on both sides of the tail while the glow in the zero order image is very much brighter on the starboard side. Only diffuse scattered light could provide equal luminosity on both sides of the tail. Our previous results (Mende et al. 1983b) already shows that the the 7619 component of the airglow is the most intense airglow component reaching several hundred kilorayleighs in the limb view.

Following the observations of the shuttle glow spectra a thruster glow experiment was carried out. In this experiment the camera was opened for 2 seconds. During the exposure a selected thruster was fired for a minimum single impulse by manual operation of another crew member. There are 6 Vernier thrusters on the orbiter. Some of them can be operated singly while others are usually operated in pairs. Four different combinations of thruster firings were performed and the results photographed. A two second duration background exposure was also taken in between each thruster firing to assure us that all thruster effects disappeared prior to the next firing. The results are shown on Figure 3 in the form of a collage of the photographic images. Note that the only thruster which has a noticeable effect on the picture background is the downward firing tail thrusters.

The time development of the thruster firings can be best studied by means of the orbiter closed circuit TV cameras. A thruster firing event documented by the orbiter TV cameras on video tape are included in Figure 4. To aid in the timing of the event a time counter which ran in seconds and one hundredth seconds was superimposed on the frames. The status of this time counter provided a unique identification of the TV frame. The first image (top left) is a background frame. The second and third images show the thrusters while in operation. The following frames show the decay of the glow on the engine pods which persists well after the thrusters had been shut off.

Figure 5 shows the thruster induced glow intensity as a function of time. This was obtained by integrating the video signal from all pixels inside of a rectangular area which includes the glow on the port side engine pods. This integrated signal was plotted on the chart recorder. Thus this video signal contains a number of relatively unknown parameters such as the signal non-linearities and the time response characteristics of the television system. Nevertheless, these effects are believed to be very small. From Figure 5 the reader can see that the thruster induced spacecraft glow takes several seconds to decay. Comparisons with similar data on STS-3 shows that the orbiter thruster decay time constant on STS-8 is about five times than that of the earlier flight. The explanation must be in the altitude difference.

DISCUSSION

Understanding of the spacecraft glow is important because it may shed light on unanticipated upper atmospheric chemical and physical processes. The spacecraft glow also has its practical significance as a contaminant to light sensitive instrumentation.

The spectral results of STS-8 are not altogether new. From previous measurements on STS-4 and STS-5 we have come to realize that the spacecraft glow had a continuum spectra and was devoid of significant lines. The present results are confirming these findings and have yielded high enough signal to noise ratio to permit quantitative interpretation of the emissivity as a function of wavelength. Preliminarily we can say that the spectra of the glow shows relatively little emission intensities below 500 nm and above this the emissions reached a peak between 600 and 700 nm. Without more quantitative densitometry it is hard to interpret the data any further. The basic shape of the spectral content is, of course, no surprise when we look at the color photos with the orange red images of the spacecraft glow. Perhaps it is even more significant to mention that there are no distinct spectral features in the spectrum. From the observation of the reflected airglow light at 762.2 nm we can see that the instrumentation is fairly sensitive to distinct line emissions, had they been present.

Our qualitative preliminary spectral data could be interpreted to be similar to the continuum spectra of NO_2 as shown by Torr (1983) and Fontijn et al. (1964), perhaps with some OH mixed in to enhance the red. There is some difficulty in the NO_2 explanation because of the emission lifetimes which can be derived from the thickness of the glow. At the altitude of the spacecraft, 200 km and above, the mean free path is several hundred meters. In order to account for the thickness of the glow layer we assume that the emitting species are formed on the surface and the emission takes place during the transit of the emitting species away from the surface. The emission is delayed due to the relatively long lifetime of the parent state. Assuming a thermal speed of the collision products of approximately 1000 m per second and a glow thickness of the order of .1 meters the lifetime of the parent state is of the order of 10^{-4} seconds. Note that if the collisions with the orbiter are elastic, Papadapolous (1983), then the velocity relative to the orbiter may be the same as the orbiter velocity (7.3 km s^{-1}). This would require the lifetime to be even shorter (~ 10^{-5}s). The lifetimes associated with the NO_2 mechanism do not agree with the observed lifetime. Our spectra seems to rule out OH as being the sole contributor in the visible through the Meinel bands as proposed by Slanger (1983).

Probably the most significant result on STS-8 is establishing that the intensity of the glow depends on the surface material. The glow in front of the black chem-glaze (carbon filled polyurethane paint) is much greater then in front of Kapton (polyimide) or aluminum samples. Thus the surface material takes an active role in the production of the glow. This should serve as a discouragment to hypotheses which maintain that the glow is generated purely by atmospheric constituents. Such was for example the originally proposed as the O_2 recombination hypothesis. Another theory is the one recently proposed by Papadapolous (1983). This suggests that the glow is excited by hot electrons which are the by-product of the Alfven critical ionization process. Although our finding creates difficulties for these type of therories it does not completely rule them out and it is still possible that the atmospheric constituents themselves are causing the glow through chemical or plasma interactions. The surfaces may still influence the intensity by acting as a catalyst. At first glance it appears that the Papadopolous mechanism could not be supported as proposed because the plasma environment should not vary from one surface sample to another. There may be still some validity in considering the Alfven critical ionization process as a contributing factor. If the source of the particles are established to be materials on the vehicle surface than we can consider larger molecules than O. Because of the size of these particles the kinetic energy is higher at the shuttle velocity of 7.3 km s^{-1} plus the thermal velocity of 1 to 2 km s^{-1} which might be sufficiently high for the critical velocity ionization to occur spontaneously without the elastic reflection postulated by Papadopolous (1983).

Most of our photography took advantage of the oblique viewing of the shuttle surfaces to maximize the intensity. A preliminary estimate of the STS-8 glow intensity would suggest between 10 and 100 kilorayleighs for these oblique views. For viewing the glow in a direction normal to the shuttle surfaces we estimate the intensity to be in the 1 to 10 kilorayleighs category. Assuming that it is of the order of 5 kilorayleighs then the total number of radiating particles is 5×10^9 per cm^{-2} of the surface area.

The oxygen density was estimated to be 2.3×10^9 cm^{-3} for the STS-8 flight (Hadine 1983 private communication). The spacecraft velocity of 7.3 km/sec yields a total O flux of 1.7×10^{15} cm^{-2}. Accordingly, if the glow is caused by the O flux incident on the spacecraft then approximately one in 10^6 O particle causes the emission of a glow photon.

It is interesting to note that the sample materials were analyzed and the mass losses due to oxidization were estimated by Leger (private communication, 1983). Accordingly, the mass loss of kapton was very large, 35% by weight of the kapton tape was gone. The loss of material of the Al or Chem-glaze samples were below measurable levels. The kapton loss was equivalent to 5×10^{-9} gm cm^{-2} sec^{-1} or $(6 \times 10^{23}/ 100??)$ about 10^{13} particles per cm^2. According to this only one out of 10^4 particles of kapton needed to produce a glow photon.

ACKNOWLEDGEMENTS

The authors would like to thank mission manager Mr. E. L. Michel of the Johnson Space Center for his efforts in organizing the STS-8 experiment. We are grateful to the flight crew of STS-8, and special thanks are due to D. C. Brandstein who took the photograph during the flight. Support of the Johnson Space Center photographic division is gratefully acknowleged. This program was supported by NASA under contract NASW-3658 and by a Lockheed independent research program.

REFERENCES

Banks, P.M., P.R. Williamson, and W.J. Raitt, Space Shuttle Glow Observations, Geophys. Res. Ltrs., 10., 118, 1983.

Fontjin A., C. B. Meyer and H. I. Schiff, Absolute Quantum Yield Measurements of the NO-O Reaction and its Use as a Standard for Chemiluminescent Reactions, J. Chem. Phys., 40, 64, 1964.

Mende, S.B., O.K. Garriott and P.M. Banks, Observations of Optical Emissions on STS-4, Geophys. Res. Ltrs., 10, 122, 1983a.

Mende, S. B.,P. M. Banks,R. Nobles,O. K. Garriott and J. Hoffman, The Measurements of Vehicle glow on the Space Shuttle, Accepted in the Journal of Rockets and Spacecraft. 1983c.

Mende, S. B.,P. M. Banks,R. Nobles,O. K. Garriott and J. Hoffman, Photographic Observations of Earth's Airglow from Space, Geophys. Res. Letrs.,Nov. 1983b.

Papadopolous K., On the Shuttle Glow (The Plasma Alternative), S. A. I. Report No. 84-147-WA, 1983.

Slanger T. G., Conjectures on the Origin of the Surface Glow of Space Vehicles, Geophys. Res. Letrs.,10,130, 1983.

Torr M. R.,Optical Emissions Induced by Spacecraft-Atmosphere Interactions, Geophys. Res. Letrs.,10, 114. 1983.

Yee, J. H., and V. J. Abreu, Visible Glow Induced by Spacecraft-Environment Interaction, Geophys. Res. Letrs.,10,126. 1983.

FIGURE CAPTIONS

Figure 1. In order to investigate the dependence of the glow intensity on the properties of the spacecraft surface materials samples were mounted on the remote manipulator system (RMS) arm. Top photograph shows the layout of the samples on the vehicle prior to flight. The samples are in the following sequence: kapton (polyimide), aluminum, black chem-glaze, aluminum, and kapton. Kapton was chosen because of its known weight loss property in space environment, aluminum was chosen because its known stability and black chem-glaze (carbon filled urethane based matt black light absorbing paint) because of its application in low light level detecting devices. Image intensified (bottom) photograph of the the RMS arm with the material samples. The glow above the chem-glaze is stronger than the glow above the other materials. Aluminum glows the least. The kaptons samples are indistinguishable from the covering material of the arm. This photograph is the first solid evidence that the spacecraft ram glow depends on the material surface properties of the spacecraft.

Figure 2. Image intensifier photograph of the shuttle tail through the objective grating. The exposure was one second duration with F/2.8. The velocity vector is in the direction of the starboard wing (left on the picture) illuminating the starboard side of the tail and the starboard engine pod. On the photograph these can be observed most clearly in the right side of the picture where the zero order image is located. The horizontal streaks on the

photographs are the first order images or spectra of stars. Some stars have both their zero order point and first order streak images in the picture. The large diffuse image a little left of the center is the first order or spectral image of the glow. Approximate wavelength scale was superimposed on the frame.

Figure 3. Collage of photographic images of attitude control thruster firings. The camera was opened for a two second duration exposure and selected thrusters were fired during the exposure. The images are the same as on Figure 2. showing the objective spectrum of the tail glow. The background however is brighter due to the thruster firings. Note that the only thruster which has a noticeable effect is the downward firing tail thrusters.

Figure 4. A schematic sketch of the location of the thrusters on the orbiter.

Figure 5. Collage of television monitor photographs of the thruster firing as recorded by the orbiter bulkhead closed circuit television cameras. Time counter in seconds and hundredth of seconds. Note that glow on engine pods is enhanced after jet firing.

Figure 6. The function of the thruster glow intensity on the engine pods as a function of time after a thruster firing. The data was taken with the orbiter bulkhead video cameras. Intensity is in arbitary units.

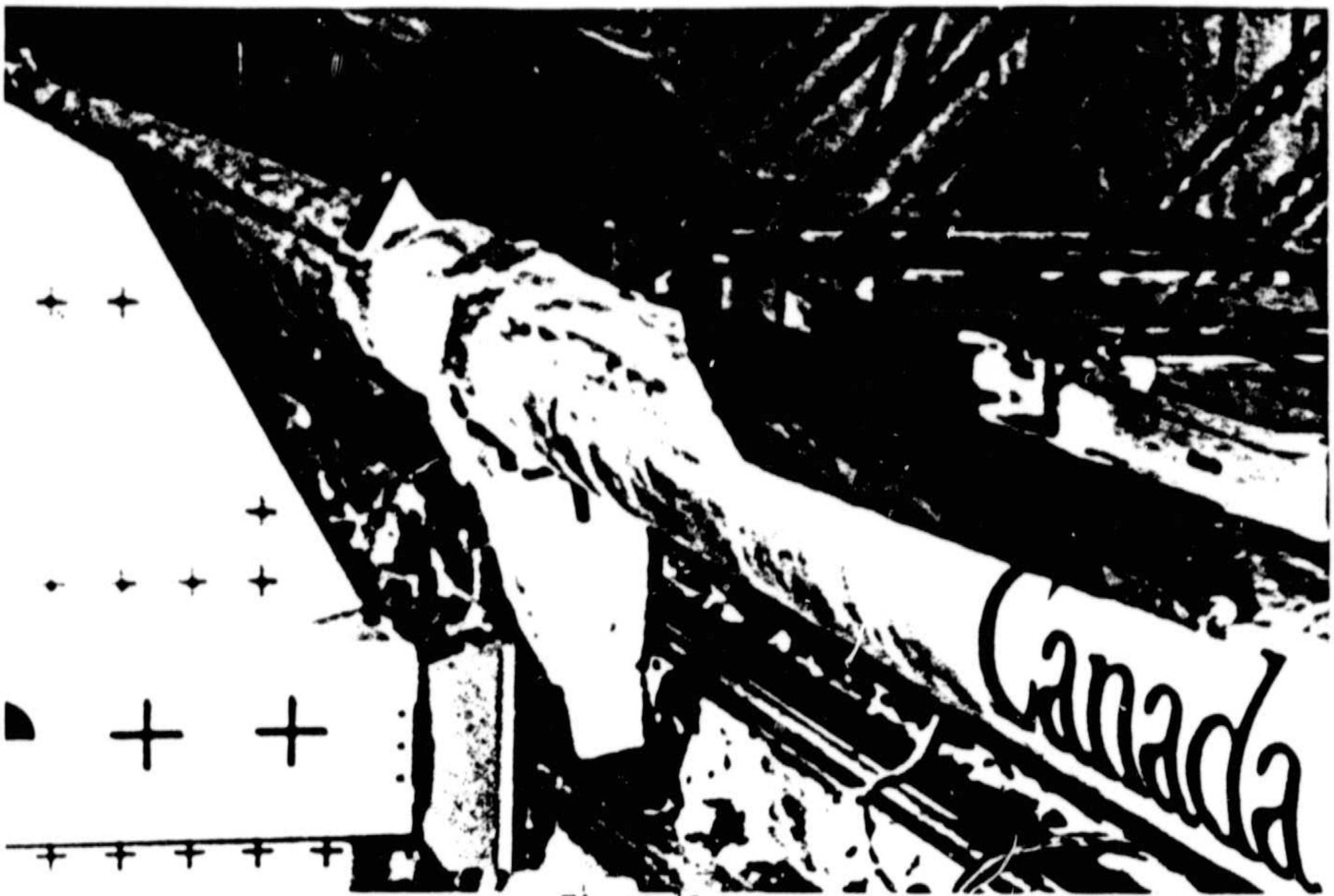

Figure 1a.

Figure 1b.

ORIGINAL PAGE
BLACK AND WHITE PHOTOGRAPH

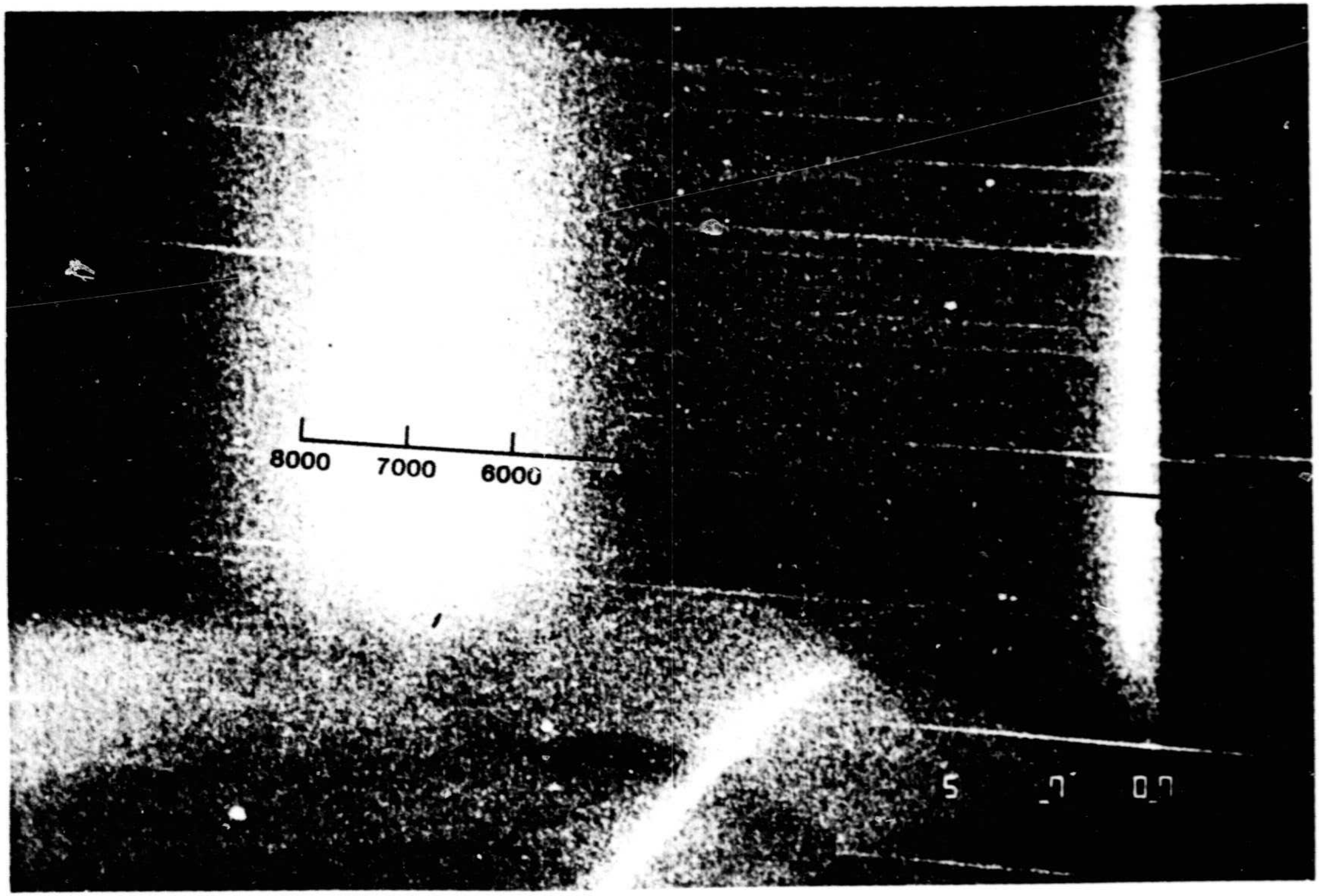

Figure 2.

THRUSTER FIRINGS

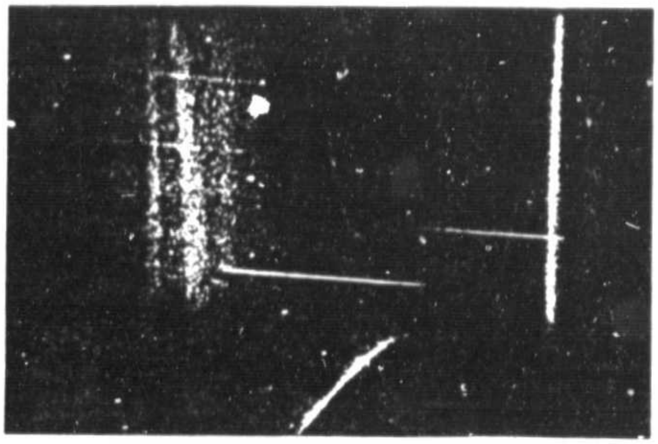

BACKGROUND

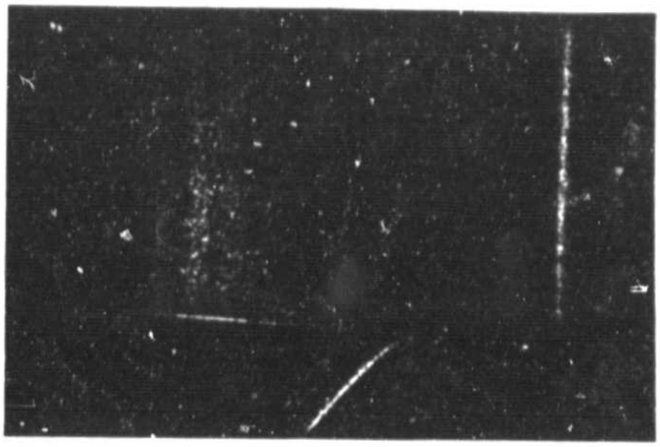

FORWARD JETS

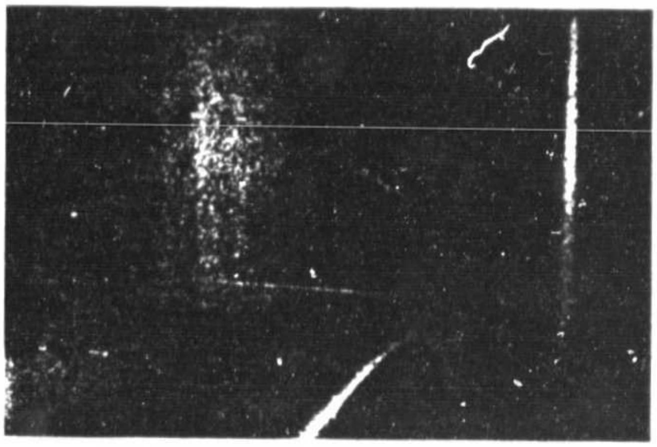

TAIL YAW JET 1

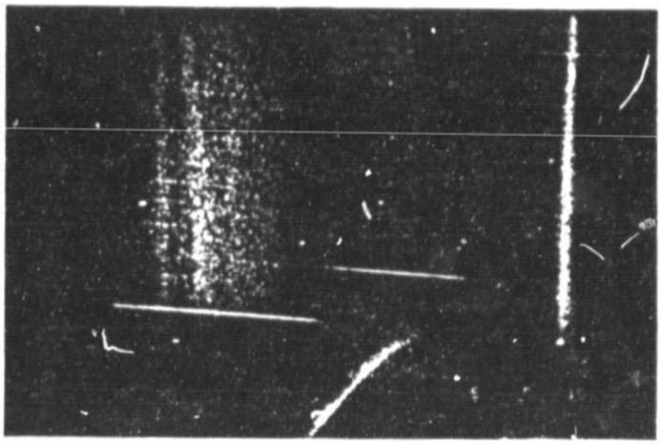

TAIL YAW JET 2

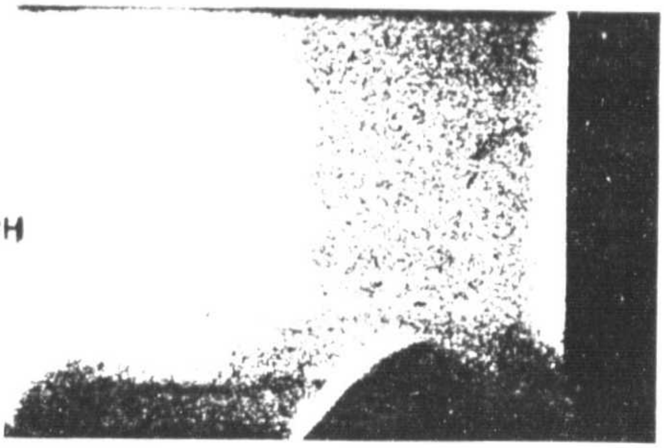

TAIL DOWNWARD JETS

Figure 3.

JET LOCATIONS

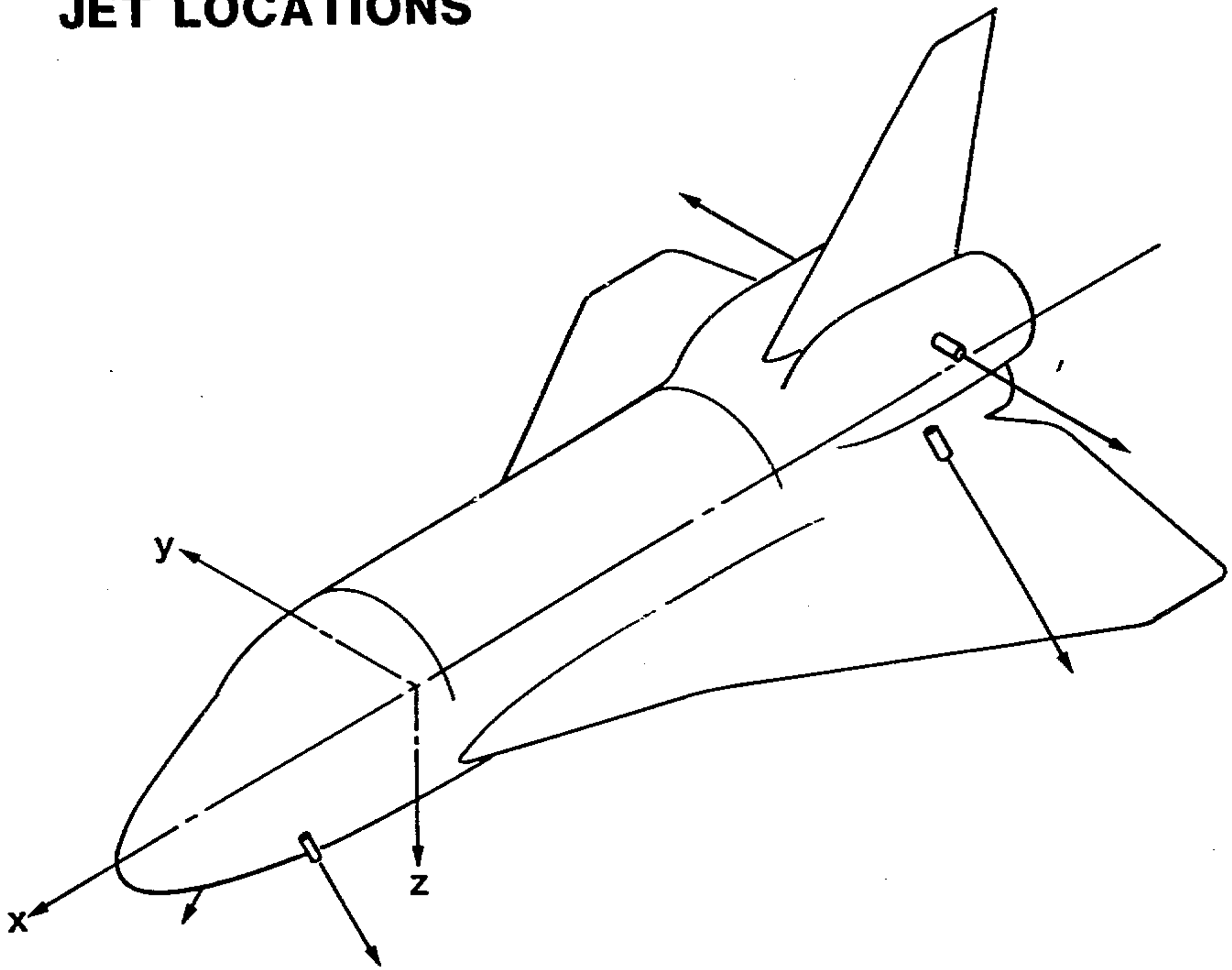

Figure 4.

THRUSTER FIRING DECAY

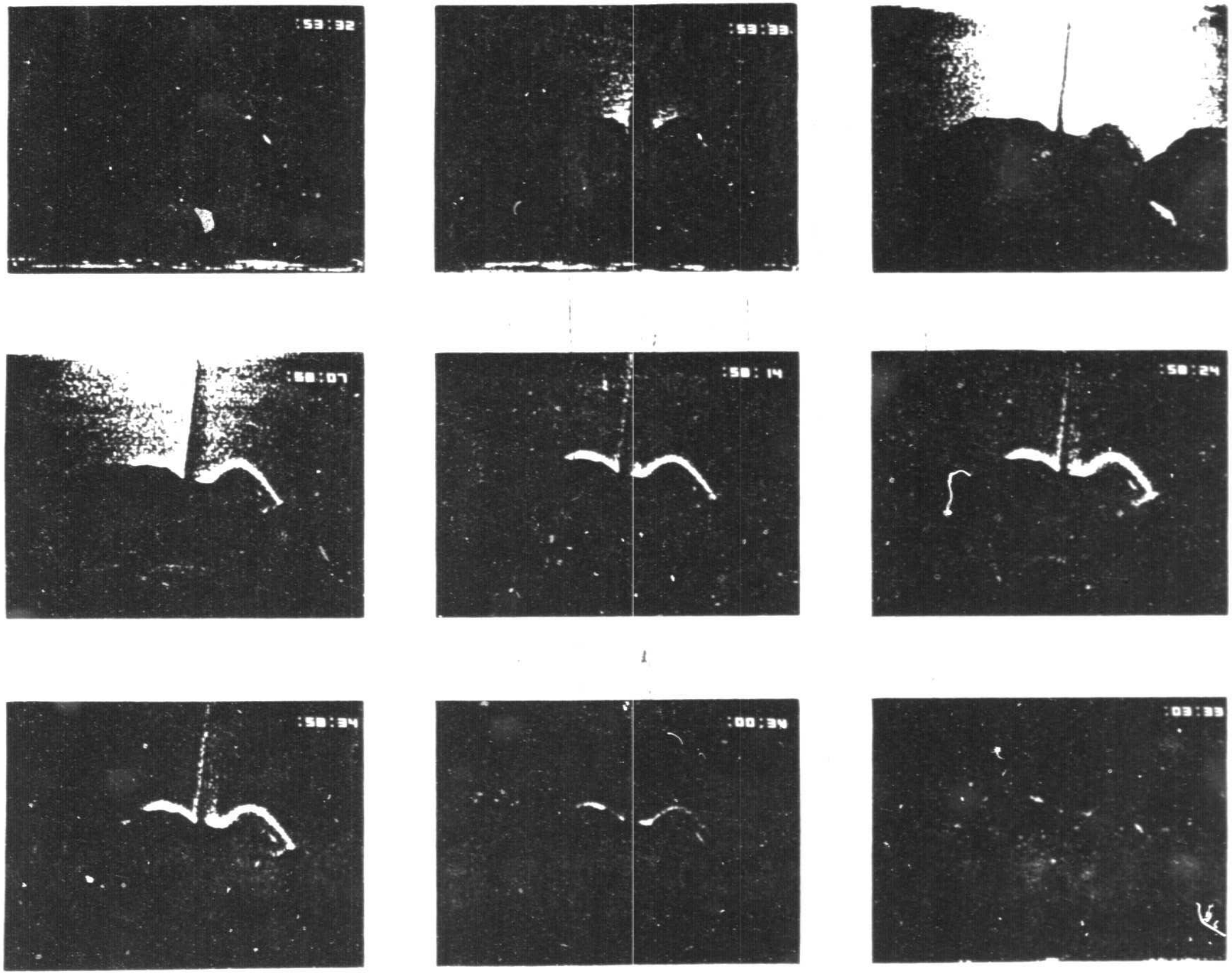

Figure 5.

TIME (s)

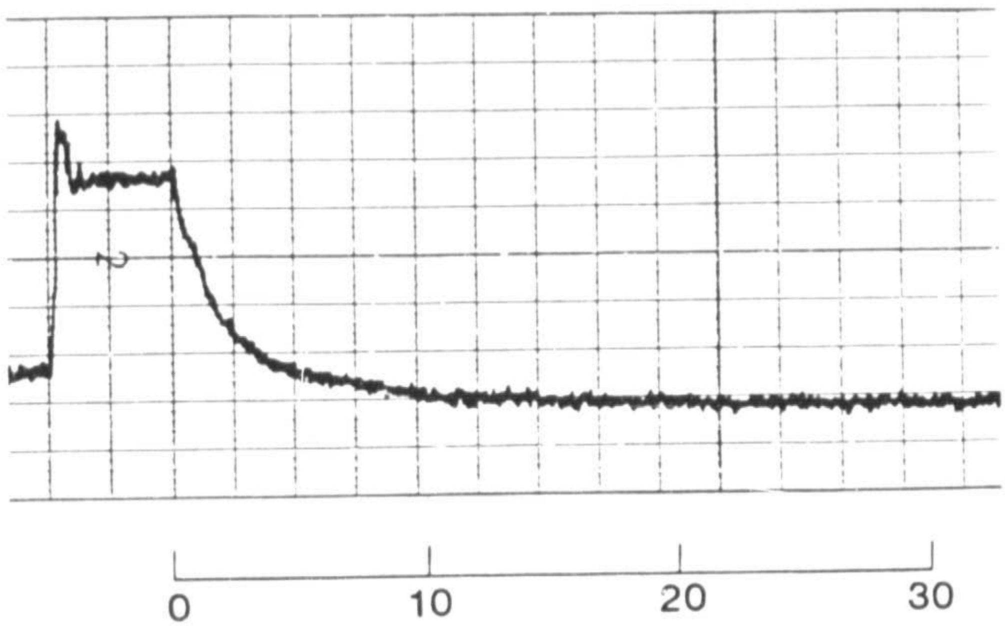

Figure 6.